Journal of Experimental Botany, Vol. 69, No. 18 pp. 4483–4493, 2018
doi:10.1093/jxb/ery240 Advance Access publication 28 June 2018
This paper is available online free of all access charges (see https://academic.oup.com/jxb/pages/openaccess for further details)

RESEARCH PAPER

Antenna proton sensitivity determines photosynthetic light harvesting strategy

Eliška Kuthanová Trsková[1,2], Erica Belgio[1,*], Anna M. Yeates[1], Roman Sobotka[1,2], Alexander V. Ruban[3] and Radek Kaňa[1,2,*]

[1] Institute of Microbiology, Academy of Sciences of the Czech Republic, Opatovický mlýn, 379 81 Třeboň, Czech Republic
[2] University of South Bohemia in České Budějovice, Faculty of Science, Branišovská 31a, 370 05 České Budějovice, Czech republic
[3] School of Biological and Chemical Sciences, Queen Mary University of London, London, UK

* Correspondence: belgio@alga.cz or kana@alga.cz

Received 7 March 2018; Editorial decision 22 June 2018; Accepted 26 June 2018

Editor: Roland Pieruschka, Forschungszentrum Jülich, Germany

Abstract

Photoprotective non-photochemical quenching (NPQ) represents an effective way to dissipate the light energy absorbed in excess by most phototrophs. It is often claimed that NPQ formation/relaxation *kinetics* are determined by xanthophyll composition. We, however, found that, for the alveolate alga *Chromera velia*, this is not the case. In the present paper, we investigated the reasons for the constitutive high rate of quenching displayed by the alga by comparing its light harvesting strategies with those of a model phototroph, the land plant *Spinacia oleracea*. Experimental results and *in silico* studies support the idea that fast quenching is due not to xanthophylls, but to intrinsic properties of the *Chromera* light harvesting complex (CLH) protein, related to amino acid composition and protein folding. The pK_a for CLH quenching was shifted by 0.5 units to a higher pH compared with higher plant antennas (light harvesting complex II; LHCII). We conclude that, whilst higher plant LHCIIs are better suited for light harvesting, CLHs are 'natural quenchers' ready to switch into a dissipative state. We propose that organisms with antenna proteins intrinsically more sensitive to protons, such as *C. velia*, carry a relatively high concentration of violaxanthin to improve their light harvesting. In contrast, higher plants need less violaxanthin per chlorophyll because LHCII proteins are more efficient light harvesters and instead require co-factors such as zeaxanthin and PsbS to accelerate and enhance quenching.

Keywords: *Chromera velia*, *in vitro* quenching, light harvesting strategy, non-photochemical quenching, NPQ kinetics, photoprotection, quenching pK_a, violaxanthin.

Introduction

Although under low light more than 83% of absorbed photons can be converted into chemical energy (e.g. Jennings *et al.*, 2005; Wientjes *et al.*, 2013), prolonged high light exposure rapidly switches photosystems to energy-dissipating states that release excess energy as heat (Demmig-Adams, 1990; Kaňa and Vass, 2008; Ruban *et al.*, 2012). The switch from light-harvesting to energy-dissipation mode has long been investigated, resulting in various models for various autotrophs (Demmig-Adams, 1990; Horton *et al.*, 1996; Kaňa *et al.*, 2012; Pinnola *et al.*, 2013; Erickson *et al.*, 2015; Büchel, 2015).

In higher plants, several processes contribute to excess light energy dissipation, but only the pH-dependent one, the

Abbreviations: CLH, *Chromera* light harvesting complex; DCCD, dicyclohexylcarbodiimide; DEPS, xanthophyll cycle de-epoxidation state; LHCII, light harvesting complex II; NPQ, non-photochemical quenching.

so-called energy-dependent quenching mechanism (non-photochemical quenching; NPQ) is considered photoprotective (Demmig-Adams and Adams, 1992; Ruban, 2013). Proof of a strict connection between NPQ and pH is that reverse ATPase activity can stimulate NPQ even in the dark (Gilmore and Yamamoto, 1992). Besides controlling xanthophyll cycle activity, in several phototrophs pH exerts a direct control on NPQ. This is thought to act via a regulation of antennas (e.g. Dekker and Boekema, 2005; Horton *et al.*, 2008; Peers *et al.*, 2009; Grossman *et al.*, 2010). Indeed, a very similar thermal dissipation process to that *in vivo* can be induced *in vitro* in purified antennas by lowering pH and detergent concentration (Ruban *et al.*, 1994*a*). Starting from this evidence, it was proposed that antenna aggregation is at the basis of the NPQ process (Horton *et al*, 1996), and subsequent findings employing liposomes started to clarify how pH and ions together with lipids and lipid to antenna ratios control the 'aggregation state' of antennas (Moya *et al.*, 2001; Kirchhoff *et al.*, 2008; Akhtar *et al.*, 2015; Kaňa and Govindjee, 2016; Natali *et al.*, 2016; Crisafi and Pandit, 2017). In higher plants, antennas are the site of energy dissipation, whilst xanthophylls and the PsbS protein seem to be simply controllers of the process (Noctor *et al.*, 1991; Walters *et al.*, 1994; Li *et al.*, 2000; Betterle *et al.*, 2009). Evidence that *npq1*, a mutant lacking zeaxanthin, and *npq4*, a mutant without PsbS, could both perform NPQ indicated their dispensability, thus placing antennas and pH as the *only* key elements of the process (Niyogi, 1999; Johnson *et al.*, 2009; Johnson *et al.*, 2011). Nevertheless, xanthophylls play an important role modulating the kinetics of NPQ activation and dissipation (Johnson *et al.*, 2010). Pre-conditioning of leaves with light exposure, for instance, makes NPQ fast and persistent because of the conversion of violaxanthin into zeaxanthin (Ruban and Horton, 1999). Zeaxanthin, a highly hydrophobic pigment, in turn, makes antennas more dehydrated and therefore sensitive to pH and prone to quench compared with violaxanthin-enriched antennas. Interestingly, this idea was put forward not only for higher plant antennas (Ruban *et al.*, 1994*a*), but also for antennas from distant organisms such as diatoms (Gundermann and Büchel, 2008), brown algae (Ocampo-Alvarez *et al.*, 2013) and alveolates (Kaňa *et al.*, 2016).

The state-of-the-art model of NPQ for plants claims that, under high light, lumen acidification induces antenna protonation, which in turn triggers protein conformational changes, aggregation and energy dissipation. However, it seems that pre-aggregation *in vivo* can affect efficiency of antenna protonation and *vice versa* (e.g. Petrou *et al.*, 2014). Optical changes induced by aggregation can be visualized spectroscopically (Lokstein *et al.*, 2002), specifically as an increase in the fluorescence yield of red-shifted emission from antennas at low temperatures (Ruban *et al.*, 1991; Bassi and Dainese, 1992; Miloslavina *et al.*, 2008; Belgio *et al.*, 2012). Based on dicyclohexylcarbodiimide (DCCD) binding and mutagenesis work (Ruban *et al.*, 1998; Belgio *et al.*, 2013; Ballottari *et al.*, 2016), it was concluded that sensors for low pH are negatively charged residues located in a lumen-exposed antenna protein loop and in the C-terminus. Once protonated, those residues become neutral, thus making the whole protein more hydrophobic and easier to aggregate and quench. Although *in vitro* fluorescence quenching as a function of pH has been observed for various types of antennas (Gundermann and Büchel, 2012; Kaňa *et al.*, 2012; Schaller-Laudel *et al.*, 2015), identification of putative protonable residues so far concerned mainly antennas from the green lineage (Ruban *et al.*, 1998; Li *et al.*, 2004; Liguori *et al.*, 2013; Belgio *et al.*, 2013; Ballottari *et al.*, 2016).

Despite the progress in our understanding of NPQ in higher plants, this subject has been less explored in algae. The alveolate *Chromera velia* represents an interesting system in this context, as it shows efficient non-photochemical quenching (Kotabová *et al.*, 2011; Quigg *et al.*, 2012; Mann *et al.*, 2014) with similarities on the one side to higher plants, and on the other to brown algae and diatoms (see below). Isolated from stony corals from Sidney harbor, this facultative symbiont is globally distributed in the marine environment at depths not exceeding 5 m (Obornik and Lukes, 2013). The phylogenic origin of the alga is complex. *C. velia* is an alveolate, and therefore closely related to dinoflagellates and other algae in the SAR clade (such as diatoms and brown algae), but all phylogenic analyses have invariably demonstrated its genuine relationship to apicomplexan parasites (Oborník *et al.*, 2016). In any case, *C. velia* is considered a 'red-clade' alga, i.e. an alga whose chloroplast was obtained by secondary endosymbiosis from a red algal ancestor (Kotabová *et al.*, 2011; Sobotka *et al.*, 2017). In *C. velia*, NPQ is connected to the xanthophyll cycle (Kotabová *et al.*, 2011) as in brown algae (Ocampo-Alvarez *et al.*, 2013); however, differing from them (Garcia-Mendoza *et al.*, 2011) but similar to diatoms (Ruban *et al.*, 2004; Lavaud and Kroth, 2006; Grouneva *et al.*, 2008), its activation is extremely fast (almost monophasic) and pH-dependent (see Belgio *et al.*, 2018).

In the present paper, we investigated the reasons for the characteristic high rate of quenching displayed by the alga. We compared the NPQ of *C. velia* with that of a higher plant (a well-known system) and showed that the mechanism of heat dissipation and in particular NPQ *activation* is different in the two evolutionarily distant phototrophs. Our data indicated that the *Chromera* light harvesting complex (CLH) is more sensitive to protons than the higher plant antenna (light harvesting complex II; LHCII). We propose that protonation of the antenna is the basis of the 'constitutively' fast NPQ found in *C. velia* and, as previously suggested for diatoms (Lavaud and Kroth, 2006; Lavaud and Lepetit, 2013), ΔpH *by itself* is important for NPQ activation. This conclusion might also explain the unusual high light acclimation strategy recently reported for *C. velia*, consisting of a decrease in reaction centers whilst still maintaining a full antenna content (Belgio *et al.*, 2018).

Materials and methods

Plant material

Chromera velia (strain RM12) was grown in artificial sea water with additional f/2 nutrients (Guillard and Ryther, 1962). Cells were cultivated in glass tubes at 28 °C, in a continuous light regime of 200 μmol m^{-2} s^{-1} while aerated with air.

Spinacia oleracia (spinach) was purchased from a local supermarket. Intact chloroplasts were prepared as previously described (Crouchman *et al.*, 2006).

Isolation of C. velia *and plant light harvesting complexes*

C. velia cells were broken and solubilized as described in Kaňa *et al.* (2016) and then loaded on a fresh, continuous 5–15% sucrose density gradient prepared using a home-made gradient maker in buffer containing 25 mM HEPES pH 7.8 and 0.04% *n*-dodecyl β-D-maltoside (β-DM). The ultracentrifugation was performed at 140 000 *g* at 4 °C for 20 h (with rotor SW28, for 40 ml tubes, of an L8-M ultracentrifuge; Beckmann, USA). The resulting band no. 2 contained a strong double band at 18 and 19 kDa, previously identified as 'fucoxanthin chlorophyll *a*/*c* binding protein (FCP)-like antenna' (Tichy *et al.*, 2013). The band analysis by Pan *et al.*, (2012) and Tichy *et al.* (2013) placed this antenna protein within the main FCP-like group of light-harvesting complexes and so it was named *Chromera* light harvesting complex (CLH).

After separation by sucrose gradient, the antenna protein was desalted using a PD10 column (GE Healthcare) in a buffer containing 20 mM HEPES (pH 7.6) and 0.01% (w/v) β-DM. Spinach LHCIIb was isolated as previously described (Ruban *et al.*, 1994*b*) and then purified, desalted and eluted in the same buffer as CLH. In both cases, antennas were isolated from samples dark-adapted for 30–45 min.

Non-photochemical fluorescence quenching in native cells and isolated chloroplasts

Chlorophyll fluorescence was measured using a double modulation fluorometer FL-3000 (Photon System Instruments, Czech Republic). A multiple turnover saturating flash was applied to measure the maximum quantum yield of the photochemistry of photosystem II (F_v/F_m) according to $(F_m-F_0)/F_m$, where the difference between the maximum (F_m) and minimum (F_0) fluorescence is used to calculate the variable fluorescence (F_v) (van Kooten and Snel, 1990). Cells were then illuminated with an orange actinic light (625 nm, 500 μmol photons m^{-2} s^{-1}), during which periodic saturating flashes were applied. NPQ was calculated as $(F_m-F_m')/F_m$ or F_m', where F_m' is the maximum fluorescence measured in the presence of actinic light. Non-photochemical quenching of fluorescence was measured in whole cells of *C. velia* (chlorophyll concentration 0.7 μg ml^{-1}) and isolated spinach chloroplasts (chlorophyll concentration 1.4 μg ml^{-1}). NPQ formation rates (NPQ as a function of time) in different xanthophyll cycle de-epoxidation states (DEPSs) were determined from the measured fluorescence traces as described in the 'Data analysis and model fitting' section.

Where indicated (Fig. 2; Supplementary Fig. S1 at *JXB* online), the effect of an uncoupler on the fluorescence quenching was examined by adding NH_4Cl (final concentration of 15 mM) at different time points of the measuring protocol.

In vitro *fluorescence quenching of antennas*

Isolated antennas (OD_{676}=1 cm^{-1}), solubilized in 0.01% DM, were diluted 20 times, while constantly stirring, in a room temperature buffer containing 10 mM sodium citrate and 10 mM Tris–HCl and adjusted with small drops of HCl to give the desired pH (for further details see Ruban *et al.*, 1994*a*; Belgio *et al.*, 2013). Chlorophyll fluorescence was continuously monitored using an FL 3000 fluorometer (PSI, Czech Republic, blue excitation at 464 nm, 184 μmol m^{-2} s^{-1}). The pK_a values for quenching kinetics were calculated as described in the 'Data analysis and model fitting' section.

Absorption measurement

Absorption spectra were recorded with a Unicam UV 500 spectrometer (Thermo Spectronic, UK).

Pigment extraction and HPLC analysis

Cells or chloroplasts were collected on GF/F filters (Whatman, UK) and soaked in 100% methanol (overnight at −20 °C) and disrupted using a mechanical tissue grinder. Filter and cell debris were removed by centrifugation (12 000 *g*, 15 min) and the supernatant used for absorbance measurements at 652, 665, and 730 nm. Chlorophyll concentration was determined according to Porra *et al.* (1989). HPLC was carried out on an Agilent 1200 chromatography system equipped with a diode array detector. Pigments were separated on a Luna Phenomenex C8 (2) column (particle size, 3 μm; pore size, 100 Å; dimensions, 100 × 4.6 mm), by applying a 0.028 M ammonium acetate–MeOH gradient (20/80) as described in (Kotabová *et al.*, 2011) and the eluted pigments were quantified at 440 nm. The de-epoxidation state of the xanthophyll cycle pigments (DEPS) was calculated as: (zeaxanthin+0.5 antheraxanthin)/(violaxanthin+antheraxanthin+zeaxanthin) (Johnson *et al.*, 2009; Kotabová *et al.*, 2011; Oborník *et al.*, 2011). For purified antennas, the same procedure was applied simply skipping the first step of filtration through GF/F filter.

Zeaxanthin enrichment

Plant chloroplasts and *C. velia* cells with a DEPS of 10% were obtained from dim-light-adapted samples (30 min). Enrichment in zeaxanthin was achieved as described previously (Ruban *et al.*, 1994*b*; Belgio *et al.*, 2014) by pre-conditioning leaves with 350 μmol photons m^{-2} s^{-1} under 98% N_2 for 20–40 min for 20% and 40% DEPS, respectively. For *C. velia*, 10 min illumination with 500 μmol photons m^{-2} s^{-1} was sufficient to obtain 40% DEPS, in agreement with what has been previously published (Kotabová *et al.*, 2011). DEPS was assessed by immediate incubation in methanol followed by HPLC analysis (see 'Pigment extraction and HPLC analysis' section).

In silico *studies*

For *in silico* studies, the LHCIIb structure resolved at 2.5 Å resolution (PDB code: 2BHW; Standfuss *et al.*, 2005) was employed. The structure of the CLH polypeptide (CveliaI_19753.t1 taken from Tichy *et al.* (2013)) was predicted using Phyre^2 (http://www.sbg.bio.ic.ac.uk/phyre2/html/page.cgi?id=index) and YASARA software (http://www.yasara.org). The protonation states of protein ionizable groups were computed in both cases using the H++ program (http://biophysics.cs.vt.edu), an automated system that calculates p*K* values of ionizable groups in macromolecules and adds missing hydrogen atoms according to the specified pH of the environment. Results shown for LHCIIb are relative to chain A, but results for chains B and C were very similar, in agreement with (Xiao *et al.*, 2012). As recommended for typical physiological conditions and deeply buried residues, the external dielectric value was set to 80, the internal dielectric value to 4, salinity to 0.15 and pH to 7.5.

Data analysis and model fitting

NPQ formation rates (NPQ in function of time; see Fig. 1) were determined using a well-established methodology valid for both algae and vascular plants (see Serôdio and Lavaud (2011) concerning the applicability of the Hill equation to NPQ in algae). Briefly, average data from three to six independent measurements of *C. velia* cells and spinach chloroplasts in different DEPSs were fitted using the sigmoidal Hill equation three-parameter implementation in SigmaPlot 12.5 (Systat Software, Inc., San Jose, CA, USA). The standard error of the estimate was between 0.02 and 0.08, meaning that ~95% of the data fell within 2% of the fitted line; moreover R^2 values were above 0.97, thus confirming the appropriateness of the approach.

In order to determine the quenching pK_a of antennas, we used a method previously established for various antennas including mutants (Ruban *et al.*, 1994*a*; Ruban and Horton, 1999; Belgio *et al.*, 2013; Zaks *et al.*, 2013). Briefly, the relationship between quenching kinetics and pH (see Fig. 4) and relative parameters (Table 1) were obtained from experiments like the one shown in Fig. 3 as follows. Quenching kinetics were calculated at each pH point by fitting the measured traces (Fig. 3) with the three-parameter hyperbolic decay function: $y=(y_0+ab)/(b+x)$ where $1/b$ represents the *rate* of the process. Then the data points from Fig. 4 were fitted by the sigmoidal Hill equation $y=[ax^h]/[c^h+x^h]$ in order to obtain Hill coefficients (h), pK_a values (c) and quenching kinetics at pH 4.97 (see also (Johnson *et al.*, 2012; Petrou *et al.*, 2014). The standard error of the estimate was again low (below 0.1) and R^2 above 0.90, confirming the validity of the approach.

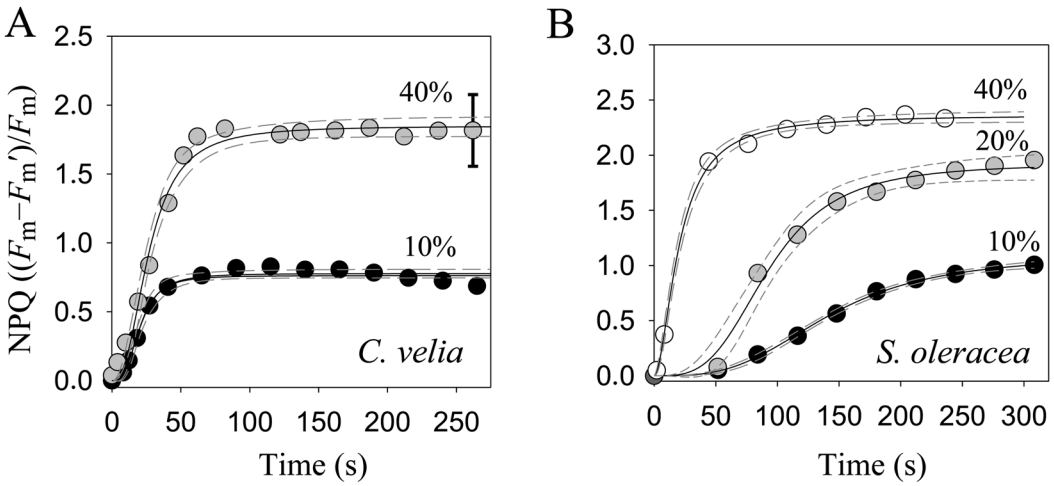

C

	NPQ_{max}	Hill coeff.	NPQ form. rate (s^{-1})
Spinach 10%	**1.09**±0.03	**3.2**±0.2	**0.01**±0.001
Spinach 40%	**2.36**±0.02	**1.8**±0.1	**0.05**±0.005
***C. velia* 10%**	**0.76**±0.02	**3.0**±0.4	**0.05**±0.01
***C. velia* 40%**	**1.90**±0.03	**2.5**±0.3	**0.04**±0.01

Fig. 1. Fast NPQ formation rate in *C. velia.* Comparison between NPQ formation in *C. velia* cells (A) and intact spinach chloroplasts (B) in different de-epoxidation states (10, 20, or 40%). Circles, average data from three to six independent measures; solid lines, fittings; dashed lines, 95% confidence intervals. The error bar shows a typical standard deviation of the data. (C) Fitting parameters and relative errors obtained using the sigmoidal Hill equation $y=[ax^b]/[c^b+x^b]$, where *a* is NPQ_{max}, *b* is the sigmoidicity parameter (Hill coefficient) and 1/*c* is NPQ formation rate (for more details, see 'Materials and methods').

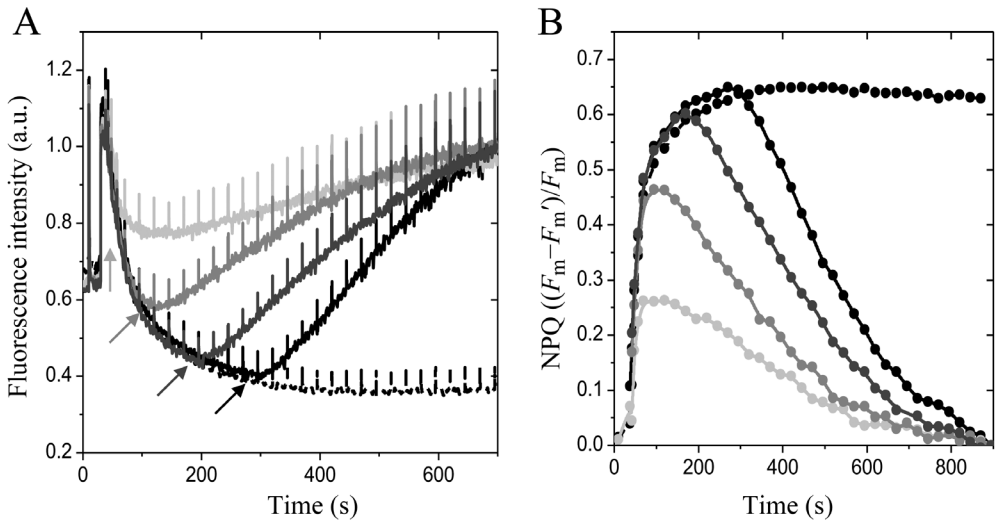

Fig. 2. NPQ of *Chromera velia* cells is ΔpH-dependent. (A) Representative fluorescence induction traces showing the effect of the uncoupler NH_4Cl on the NPQ of *C. velia* cells. Dashed black, control (no NH_4Cl); light gray, NH_4Cl added after 45 s; medium gray, uncoupler added after 99 s; dark gray, uncoupler added after 198 s; solid black, uncoupler added after 297 s. The actinic light intensity was 500 μmol m^{-2} s^{-1}. Samples were dark adapted for 30 min before measurements. Care was taken to ensure that the sample was efficiently stirred throughout the whole experiment. For further information, see 'Materials and methods'. (B) NPQ ($(F_m–F_m')/F_m$), calculated from the relative fluorescence traces shown in (A). (This figure is available in colour at JXB online.)

Results

The kinetics of non-photochemical quenching (NPQ) activation were studied for *C. velia* in different xanthophyll de-epoxidation states (DEPSs) and compared with that of *Spinacia oleracea* (spinach) (Fig. 1). NPQ formation rate positively correlated with the DEPS in spinach as 10, 20, and 40% de-epoxidation yielded significantly different NPQ formation rates of 0.006, 0.011, and 0.05 s^{-1}, respectively (Fig. 1B), in agreement

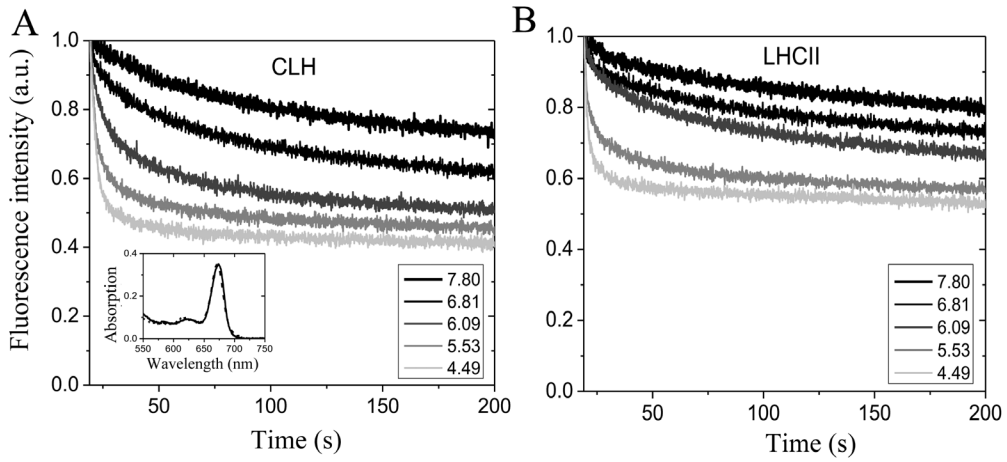

Fig. 3. Quenching of *Chromera velia* antennas is highly sensitive to pH. Representative fluorescence time course of CLH (A) and LHCII (B) as a function of pH. Samples were injected into a buffer containing 0.0005% β-DM, 10 mM HEPES and 10 mM sodium citrate (final concentrations). Each buffer had been HCl-buffered to the pH indicated in the figure, prior to sample injection. Data were normalized to the fluorescence maximum. Inset: absorption spectrum of CLH at high (solid line, pH 7.8) and low (dashed line, pH 4.5) pH. (This figure is available in colour at JXB online.)

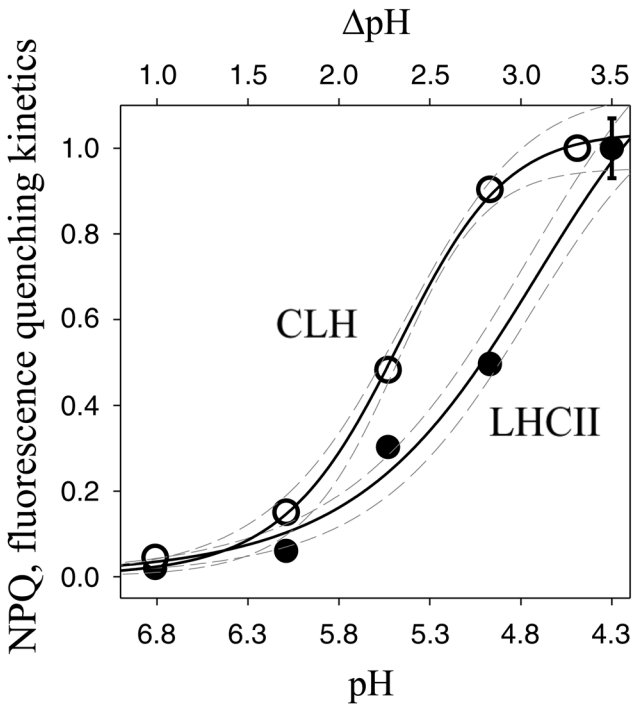

Fig. 4. Comparison of pH titration curves for fluorescence quenching of LHCII and CLH. The relationship between percentage of quenching and pH was obtained from traces like those shown in Fig. 3 fitted as described in the 'Data analysis and model fitting' section of 'Materials and methods', using a previously established model (see e.g. Ruban and Horton 1999). Circles, mean averages from at least three independent replicates; solid lines, fittings; dashed lines, 95% confidence intervals. The error bar shows typical standard deviation.

with current NPQ models and previous results from various phototrophs (see e.g. (Demmig-Adams, 1990; Ruban *et al.*, 1994*b*; Jahns and Holzwarth, 2012; Goss and Lepetit 2015). In contrast, NPQ in *C. velia* formed quickly regardless of the de-epoxidation state (Fig. 1A). Values between 0.04 and 0.05 s^{-1} were thus found for both 10 and 40% DEPS, showing fast NPQ formation, independent of xanthophyll content (Fig. 1C).

The lack of an evident kinetic effect of xanthophylls in *C. velia* can also be seen from the *shape* of the NPQ formation curve. Whilst in spinach the increase in zeaxanthin (zea) concentration from 10 to 40% reduced curve sigmoidicity from 3.2 to 1.8 (Fig. 1B; Table S1), in *C. velia* no evident change could be seen (Fig. 1A) and the Hill coefficients were not significantly different in the two conditions (3.0 ± 0.4 *versus* 2.5 ± 0.3; see Supplementary Table S1). The increased de-epoxidation (from 10% to 40%; Fig. 1A), therefore, did not seem to affect NPQ kinetics as strongly as in spinach, but it stimulated the total NPQ (NPQ_{max}; see Table S1). This is in agreement with a previous report (Kotabová *et al.*, 2011) showing NPQ enhancement by zeaxanthin in *C. velia*.

In *C. velia*, NPQ was induced almost instantaneously with the turning on of the actinic light, and we therefore used NH_4Cl to investigate the possibility that lumen acidification was the basis of fast NPQ. As with spinach, in *C. velia* NH_4Cl reversed fluorescence quenching independent of its addition time during irradiation (Fig. 2A), proving a strict link between protons and NPQ in *C. velia*. However, the kinetics of NPQ relaxation at different time points were very different from each other and from those of spinach (Supplementary Fig. S1A). Whilst in spinach NPQ relaxed almost immediately after NH_4Cl injection, with 70% fluorescence recovery within 10 s, it took at least 500 s to achieve a similar recovery in *C. velia* (Fig. 2B). Interestingly, in *C. velia*, the later NH_4Cl was added, the faster NPQ relaxed (Fig. 2B). This is in strict contrast to higher plants (Supplementary Fig. S1B), where faster relaxation kinetics were observed at the beginning of NPQ formation (see e.g. Fig. 3A in (Ruban *et al.*, 2004), suggesting a different sensitivity of NPQ to lumen acidification. The connection between NPQ and protons was further investigated *in vitro* using isolated antennas.

'Fluorescence quenching titration' is an efficient way to systematically study the pH dependency of quenching *in vitro*, by injecting purified antennas into buffers of increasingly acidic pH (Ruban *et al.*, 1994*b*; Wentworth *et al.*, 2000; Kaňa *et al.*, 2012; Belgio *et al.*, 2013). This method was employed

to assess the hypothesis that faster NPQ activation (Fig. 1) related to antenna protonation, rather than to zeaxanthin content. Therefore LHCII and CLH complexes were isolated from dark-adapted material and the absence of zeaxanthin was confirmed by HPLC analysis (see Supplementary Table S1 at *JXB* online).

Upon injection, CLH displayed a progressive quenching proportional to the acidity of the buffer (Fig. 3A). Sample integrity was constantly monitored by absorption spectroscopy (Fig. 3, inset) and by reversibility of the quenching after detergent addition (data not shown). Besides the general similarity of the process, pointing to a fundamentally conserved quenching mechanism, the differences between the two types of sample are notable. At each pH value, fluorescence quenching was consistently higher in CLH compared with LHCII, with the biggest difference found around pH 6.0. From the traces in Fig. 3, a titration curve of quenching kinetics as a function of pH was constructed (Fig. 4). It shows that, to attain the same rate of fluorescence quenching, a lower pH is required in LHCII compared with CLH. In particular, almost 50% of maximum quenching rate was observed at pH 5.5 in CLH, whilst a pH of 5.0 was necessary to get the same quenching rate in spinach. Similarly, CLH showed almost the maximum quenching rate (90 ± 5%) at pH 4.97, whereas for LHCII it was only 50%. This was reflected in a shift by 0.5 pH unit to higher values in the calculated quenching pK_a of CLH compared with LHCII, i.e. from 5.5 ± 0.1 to 5.0 ± 0.1 (Table 1). The pK_a value for LHCII was in good agreement with that previously reported (see e.g. pK_a=4.9 in Petrou *et al.* (2014)). The Hill coefficient for CLH was not significantly different from that of LHCII (7.2 ± 1.9 and 7.5 ± 1.1 for LHCII and CLH, respectively; Table 1) and in both cases they were higher than those for *in vivo* quenching (see Fig. 1), consistent with the absence of zeaxanthin (see Supplementary Table S1 and Discussion). In summary, the shift in quenching pK_a confirmed a higher proton sensitivity of CLH compared with LHCII, independent of xanthophylls.

In order to address possible reasons behind the higher pH sensitivity found in CLH, a comparative *in silico* analysis was conducted using the amino acid sequences of CLH and LHCII (Supplementary Fig. S2). A schematic overview of the two proteins is presented in Supplementary Fig. S3. We have explored in particular the protein lumenal loop to identify residues that are protonable within the physiological range. The protein structure predicted for CLH is presented in Fig. 5. We found 24 negatively charged amino acidic residues in total (i.e. aspartic and glutamic acids) in CLH, four of which are located in the luminal loop (Glu-93, Asp-107, Asp-113, Asp-119) and one in the C-terminus (Glu-205).

The estimated *in situ* pK_a values were calculated and compared with LHCII (2.5 Å resolution structure from Standfuss *et al.* (2005)) and are presented in Table 2. Results for LHCII are in good agreement with a previous report (Xiao *et al.*, 2012), where two residues in particular (Glu-107 and Asp-215) were indicated as putative pH sensors for NPQ as their quenching pK_a values are within the thylakoid physiological range (3.9–7.5). The same analysis applied to CLH revealed the presence of three plausible protonable residues: Asp-107, Asp-119 and Glu-205 (see Table 2, Fig. 5 right). Furthermore, their pK_a values were shifted to higher pH values compared with LHCII, confirming that the lumenal loop is more sensitive to protonation in CLH (see Asp-107, Asp-119 and Glu-205 and their pK_a in Table 2).

An overall comparison between LHCII and CLH protein structures (Table 3) indicated that, despite a similar number of total protonable residues (~11.4–11.5% in both cases), CLH displayed a lower protein charge than LHCII at pH 7.6, that is −6 *versus* −24, respectively. This means that LHCII tends to be more charged than CLH and a stronger protein–protein repulsion is expected for LHCIIs at pH 7.6 (see Discussion). In agreement with this, the CLH isoelectric point was ~0.4 higher than LHCII, implying that ~30 times fewer protons are required to neutralize negatively charged residues compared with LHCII. In summary, the *in silico* results supported the experimental data well and provided theoretical explanations for the faster, more efficient quenching found for CLH.

Discussion

In the present paper, we investigated reasons for fast NPQ activation in *C. velia*. In higher plants, the kinetics of NPQ induction are influenced by xanthophyll composition (Fig. 1B). Demmig-Adams (1990) was the first to provide evidence for a connection between the xanthophyll cycle and NPQ. She showed that the conversion of violaxanthin into zeaxanthin, stimulated under light by lumen acidification, strongly enhanced NPQ. Later it was noticed (Ruban and Horton, 1999) that the NPQ of zeaxanthin-enriched samples was much faster, as zeaxanthin changed the NPQ dependency (cooperativity) as a function of ΔpH, from sigmoidal (violaxanthin) to hyperbolic (zeaxanthin) (see also Horton *et al.*, 2000; Johnson *et al.*, 2009). Here, we confirmed with a control sample (spinach) that the transition into the quenched state is slower for leaves enriched in violaxanthin compared with zeaxanthin (Fig. 1B) as the Hill coefficient

Table 1. pH versus quenching titration curve fitting parameters in CLH and LHCII

Sample	Hill coefficient	Estimated pK_a	Quenching kinetics at pH 4.97
LHCII	7.2 ± 1.9	5.0 ± 0.1	0.50 ± 0.01
CLH	7.5 ± 1.1	5.5 ± 0.1	0.90 ± 0.05

Titration parameters were determined by fitting measured traces like those represented in Fig. 3 as described in the 'Data analysis and model fitting' section of 'Materials and methods'. Standard fitting errors were provided by SigmaPlot software. (For more details, see Ruban *et al.* 1994*a*; Ruban and Horton 1999; Petrou *et al.* 2014.)

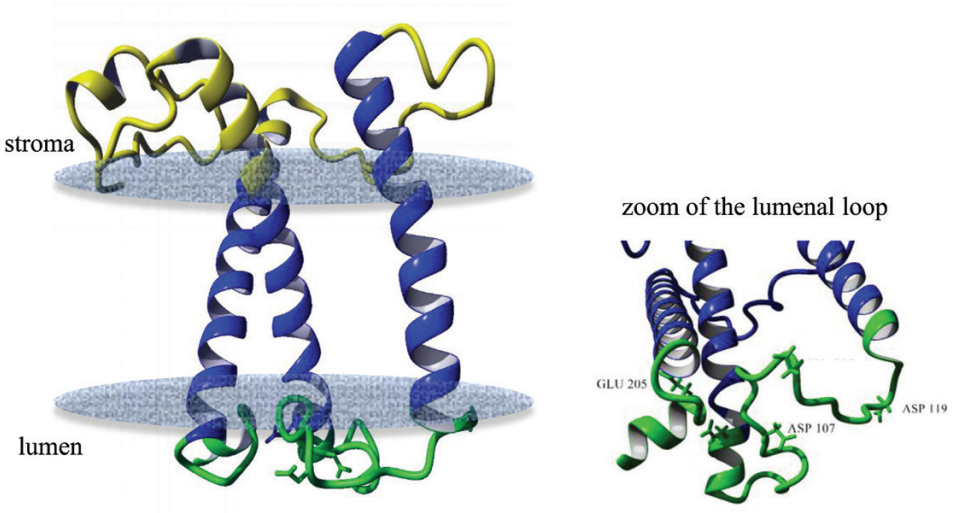

Fig. 5. Predicted protein structure for CLH. Predicted structure of the CLH antenna based on sequence homology with LHCII. A zoom of the stranded lumenal loop is shown on the right. The putative residues involved in triggering NPQ are labelled in black. Blue, transmembrane helices; green, lumenal loop region; yellow, stromal loop. For the prediction of protein structure and the pK_a of residues, YASARA and H++ programs were used, respectively.

Table 2. List of protonable lumenal loop residues (Glu, Asp) predicted by the H++ program for LHCII and CLH antenna proteins

LHCII		CLH	
Residue	**pK_a**	**Residue**	**pK_a**
Glu-94	1.5	Glu-93	1.0
Glu-107	**4.4**	**Asp-107**	**5.9***
Asp-111	3.4	Asp-113	2.9
Glu-207	2.9	**Asp-119**	**3.9***
Asp-211	3.5	Lys-211	7.4
Asp-215	**5.3**	**Glu-205**	**>7***

The putative residues that can be protonated within the physiological pH range (3.9–7.5) are in shown bold. Residues in CLH with a higher pK_a than LHCII have been marked with an asterisk. Set values in the simulation were: for internal dielectric, 4; external dielectric, 80; and salinity, 0.15; in agreement with Xiao *et al.* (2012). Predicted sequences and protein structures are shown in Supplementary Figs S2 and S3, respectively.

decreased in the presence of zeaxanthin. In *C. velia* however, we found a different behavior. Although NPQ was greater in zeaxanthin-enriched samples, confirming the first observations (Kotabová *et al.*, 2011), its *rate* was insensitive to xanthophyll composition (Fig. 1A, C), indicating that the reason for the fast NPQ in *C. velia* resided elsewhere. The NH_4Cl-infiltration experiment (Fig. 2) following the procedure of Ruban *et al.* (2004) and Lavaud *et al.* (2002), suggested that fast NPQ related to lumen acidification and protons. Incomplete diffusion of the uncoupler was in fact ruled out by previous evidence of efficient NH_4Cl penetration in *C. velia* cells (see Fig. 4b in Belgio *et al.*, 2018). The titration of NPQ as a function of pH confirmed that CLH was significantly more sensitive to protons than LHCII (Figs 2, 3). Most importantly, the *rate* of quenching was increased, especially between pH 5 and 6.5. Within this pH range a very rapid quenching formed almost instantly upon injection of a CLH sample (Fig. 3A). This resulted in a shift in quenching pK_a of CLH to higher pH values than LHCII (Table 1). Therefore, to attain 50% of maximum quenching kinetics, a 0.5 unit lower pH value (corresponding to 3.16 times more protons) was required for LHCII than CLH, indicating that the latter had an increased sensitivity to acidification. The high level of structural similarity between CLH and LHC protein families (Pan *et al.*, 2012; Tichy *et al.*, 2013; see also Supplementary Fig. S3) prompted an *in silico* comparison between lumenal loop residues. The analysis identified five protonable (i.e. negative) residues in the lumenal loop of CLH (Table 2). Three of them were predicted to be protonable within the physiological range (assuming a chloroplast lumen pH ranging between 3.9 and 7.5 (Peltier *et al.*, 2002). Compared with the corresponding residues in LHCII, the quenching pK_a values of these three residues are significantly higher in CLH (Table 2), which is consistent with the shift in the quenching pK_a found from experimental data (Fig. 4). We propose that during lumen acidification and *in vitro* quenching (Fig. 3), these residues shift from negative to neutral (i.e. become protonated) and this occurs earlier (i.e. at higher pH values) in CLH than in LHCII. This mechanism would explain the faster quenching (Fig. 3) and the shift to higher values of CLH quenching pK_a found experimentally (Fig. 4). Interestingly, the pK_a of Lys-211 (which in standard conditions has a pK_a of 10.67) was found to be reduced to 7.4 in CLH (Table 2). If confirmed by further studies, this means that this lumenal loop residue can also be protonated during lumen acidification and therefore might play a role in NPQ activation in *C. velia*. The comparison between LHCII and CLH (Table 3) indicated also that the algal antenna is less charged at physiological pH than LHCII. As protein clustering proved to be crucial for efficient quenching of LHCII (Betterle *et al.*, 2009; Johnson *et al.*, 2011; Belgio *et al.*, 2012; Petrou *et al.*, 2014), an overall less charged protein like CLH could be more prone to aggregate and therefore quench more easily, due to a minor protein–protein electrostatic repulsion. The predicted isoelectric point is consistent with this. For CLH, in fact, a ~0.4 lower p*I* was found (Table 3), corresponding to 30–40 less protons required for charge shielding. Considering the *in vitro* and *in silico* results together, we suggest that the increased NPQ formation kinetics relate to inbuilt antenna properties, in terms of

both a higher number of lumen-exposed protonable residues and an overall increased protein hydrophobicity. We hypothesize that this applies also to other similar antennas, such as diatom FCPs. In fact, although CLH binds only chlorophyll *a* and xanthophylls (see Kotabová *et al.*, 2011), due to its structural properties, this protein was classified as 'FCP-like', i.e. closely related to antennas from dinoflagellates, brown algae, and diatoms (Lepetit *et al.*, 2010; Pan *et al.*, 2012; Tichy *et al.*, 2013). Moreover diatoms can also be characterized by fast NPQ activation (Ruban *et al.*, 2004; Lavaud and Kroth, 2006; Grouneva *et al.*, 2008).

It was experimentally shown for brown algae (Nitschke *et al.*, 2012), alveolates (Belgio *et al.*, 2018), and other microalgae (Goss and Jakob, 2010) that the habitat and particularly the light conditions affect NPQ capabilities of algae from the SAR clade. As a coral symbiont, *C. velia* is expected to be mainly exposed to rather 'moderate' light intensities.

Table 3. Comparison of total charges between LHCII and CLH

	LHCII	CLH
Protonable residues	25/218 (11.5%)	24/211 (11.4%)
p*I*	4.61	4.97
Charge at pH 7.6	–24	–6

Total number of protonable residues, the isoelectric point (p*I*) and the total protein charge of LHCII and CLH antenna proteins, as predicted by the H++ program. Relative sequences and protein structures are shown in Supplementary Figs S2 and S3, respectively.

However, as this organism can be also found 'free-living' outside the coral, at depths of 3–5 m, light intensities of up to 1000 μmol m^{-2} s^{-1} are normally experienced on a sunny day (Behrenfeld *et al.*, 1998; Oborník *et al.*, 2011). We can speculate that, due to fast quenching of antennas, in *C. velia* there was no selective pressure towards proteins capable of enhancing NPQ rate such as PsbS or Lhcsr (Pan *et al.*, 2012). These proteins in fact have a role as NPQ enhancers in vascular plants and green microalgae, respectively (Goss and Lepetit 2015). Spinach and *C. velia* seem therefore to have evolved very different 'antenna behaviors' in relation to different acclimation strategies. They can be summarized as follows (Fig. 6):

- *Chromera velia* carries antenna proteins that are 'natural quenchers'; PsbS, a strong NPQ enhancer (Li *et al.*, 2000), is absent (Pan *et al.*, 2011) and the thylakoid membrane is highly enriched in violaxanthin, an 'anti-quenching' pigment (Kaňa *et al.*, 2016). As a consequence its NPQ kinetics are characterized by fast formation/slow relaxation.
- Higher plant antenna proteins, here represented by spinach LHCII, are 'natural light harvesters', so PsbS is required for effective but in particular *fast* quenching (Johnson and Ruban, 2011) and little or no free violaxanthin is present the membranes (Dall'Osto *et al.*, 2010; Xu *et al.*, 2015). The NPQ kinetics are characterized by slow formation/fast relaxation.

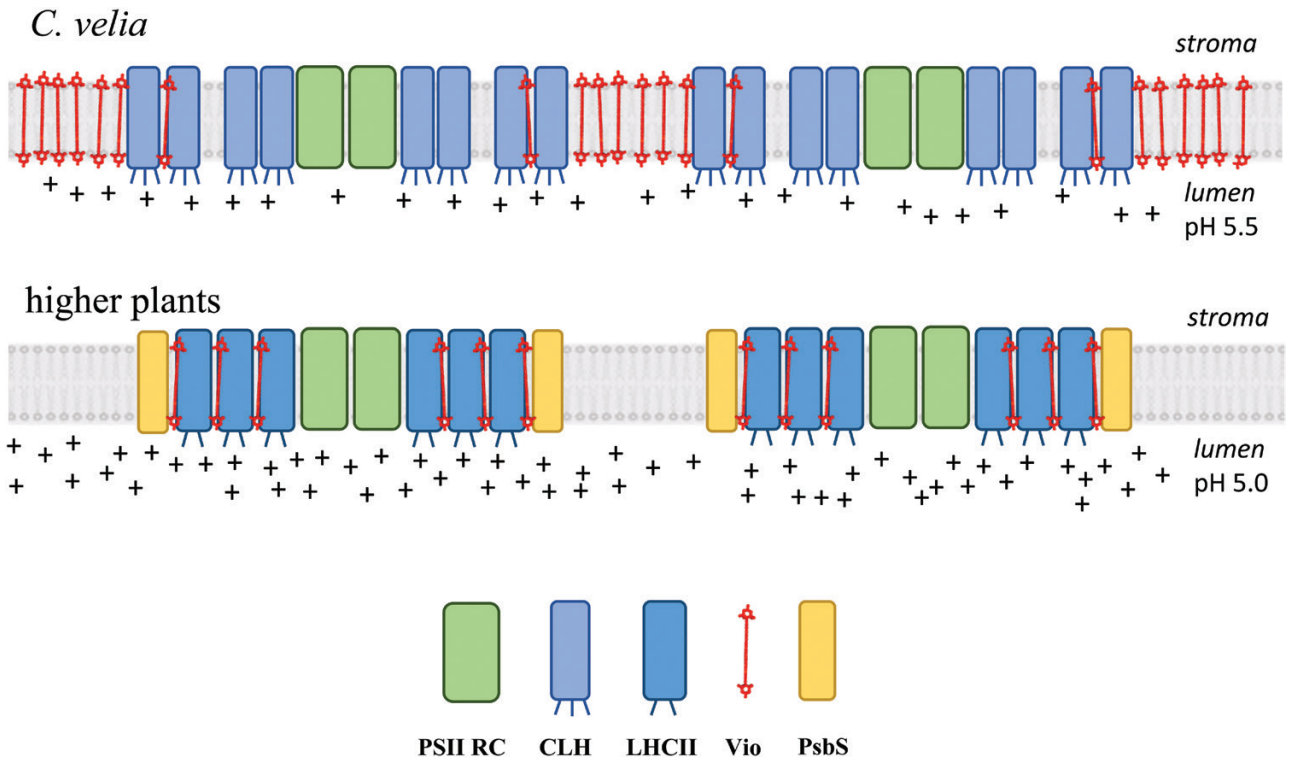

Fig. 6. Scheme showing the different light harvesting strategies of *C. velia* and higher plants. The *C. velia* thylakoid membrane carries CLH proteins that are 'natural quenchers' with three protonable lumen-facing residues, D107, D119, and E205 (indicated by small protrusions). The membrane is highly enriched in unbound, 'anti-quenching', violaxanthin pigments, and PsbS protein is absent. The higher plant thylakoid membrane supports the LHCII protein, a 'natural light harvester' with two protonable lumen-facing residues. PsbS protein is required for effective quenching, and the amount of unbound violaxanthin in the membrane is negligible. The scheme does not represent real stoichiometries/proportions. For more details, see main text.

In this scenario, 'free' violaxanthin plays a role of quenching inhibitor, particularly important for *C. velia* and less crucial for LHCII. A similar role of violaxanthin was previously suggested for some brown algae (Ocampo-Alvarez *et al.*, 2013). It explains the abundance of violaxanthin in algae like *C. velia*, where the violaxanthin to Chl *a* ratio is ~0.36 (mol mol^{-1}), ~8 times higher than in plants (see e.g. Kotabová *et al.*, 2011), which is supported by work showing quenching modulation by 'free', i.e. not firmly bound to protein, xanthophylls (Ruban *et al.*, 1994*a*; Lepetit *et al.*, 2010; Mann *et al.*, 2014; Xu *et al.*, 2015; Kaňa *et al.*, 2016).

Finally, the model presented (Fig. 6) provides an explanation also for the unusual acclimation strategy observed in *C. velia*: whilst plants (carrying 'natural harvester' antennas) protect themselves from high light by reducing their antenna size (see Kouřil *et al.*, 2013), in *C. velia* (characterized by 'natural quencher' antenna proteins) the antenna size is unaffected even after days of exposure to high light (Belgio *et al.*, 2018). This evidence, at first puzzling, seems now more logical in view of the results presented here.

Conclusions

In conclusion, we have shown a similar quenching mechanism in antennas from a higher plant compared with those from an alveolate. In both cases the trigger is low pH and the likely sensors are protonable lumenal residues. However, the actual sensitivity to lowering pH is different for the two proteins as CLH is more sensitive to protons than LHCII. We propose that this is due to subtle differences in the amino acid composition of the protein lumenal loop. As a result, CLH switches into a dissipative quenched state more easily than LHCII and therefore the higher plant antenna protein can be considered a 'natural light harvester' whilst the CLH protein is a 'natural quencher'.

Supplementary data

Supplementary data are available at *JXB* online.

Fig. S1. NH_4Cl induces fast NPQ relaxation in spinach chloroplasts.

Fig. S2. Sequence of LHCIIb and CLH used in the present study.

Fig. S3. Schematic overview of LHCII (left) and CLH (right) antenna protein structures used in the present study.

Table S1. Pigment composition of antennas isolated from *C. velia* and spinach.

Acknowledgements

This research project was mainly supported by The Czech Science Foundation GAČR (Grantová agentura České republiky) 17-02363Y (EB). Further support was from the Institutional project Algatech Plus (MSMT LO1416) from the Czech Ministry of Education, Youth and Sport. AVR was supported by The Royal Society Wolfson Research Merit Award. The authors thank Dr Petra Ungerer for LHCIIb protein preparation and Mr Filip Charvát for technical help during HPLC sample preparation.

Author contributions

RK, EKT and EB conceived the project; EKT and EB performed the experiments and analyzed the data; AMY provided HPLC technical assistance; RS provided experimental advice concerning protein isolation; EB, RK and EKT wrote the article with contributions from all the co-authors; EB, EKT and AMY prepared the Figures. AVR supervised and complemented the work.

References

Akhtar P, Dorogi M, Pawlak K, Kovács L, Bóta A, Kiss T, Garab G, Lambrev PH. 2015. Pigment interactions in light-harvesting complex II in different molecular environments. The Journal of Biological Chemistry **290,** 4877–4886.

Ballottari M, Truong TB, De Re E, Erickson E, Stella GR, Fleming GR, Bassi R, Niyogi KK. 2016. Identification of pH-sensing sites in the light harvesting complex stress-related 3 protein essential for triggering non-photochemical quenching in *Chlamydomonas reinhardtii*. The Journal of Biological Chemistry **291,** 7334–7346.

Bassi R, Dainese P. 1992. A supramolecular light-harvesting complex from chloroplast photosystem-II membranes. European Journal of Biochemistry **204,** 317–326.

Behrenfeld MJ, Prášil O, Kolber ZS, Babin M, Falkowski PG. 1998. Compensatory changes in Photosystem II electron turnover rates protect photosynthesis from photoinhibition. Photosynthesis Research **58,** 259–268.

Belgio E, Duffy CD, Ruban AV. 2013. Switching light harvesting complex II into photoprotective state involves the lumen-facing apoprotein loop. Physical Chemistry Chemical Physics **15,** 12253–12261.

Belgio E, Johnson MP, Jurić S, Ruban AV. 2012. Higher plant photosystem II light-harvesting antenna, not the reaction center, determines the excited-state lifetime—both the maximum and the nonphotochemically quenched. Biophysical Journal **102,** 2761–2771.

Belgio E, Kapitonova E, Chmeliov J, Duffy CD, Ungerer P, Valkunas L, Ruban AV. 2014. Economic photoprotection in photosystem II that retains a complete light-harvesting system with slow energy traps. Nature Communications **5,** 4433.

Belgio E, Trsková E, Kotabová E, Ewe D, Prášil O, Kaňa R. 2018. High light acclimation of *Chromera velia* points to photoprotective NPQ. Photosynthesis Research **135,** 263–274.

Betterle N, Ballottari M, Zorzan S, de Bianchi S, Cazzaniga S, Dall'osto L, Morosinotto T, Bassi R. 2009. Light-induced dissociation of an antenna hetero-oligomer is needed for non-photochemical quenching induction. The Journal of Biological Chemistry **284,** 15255–15266.

Büchel C. 2015. Evolution and function of light harvesting proteins. Journal of Plant Physiology **172,** 62–75.

Crisafi E, Pandit A. 2017. Disentangling protein and lipid interactions that control a molecular switch in photosynthetic light harvesting. Biochimica et Biophysica Acta **1859,** 40–47.

Crouchman S, Ruban A, Horton P. 2006. PsbS enhances nonphotochemical fluorescence quenching in the absence of zeaxanthin. FEBS Letters **580,** 2053–2058.

Dall'Osto L, Cazzaniga S, Havaux M, Bassi R. 2010. Enhanced photoprotection by protein-bound vs free xanthophyll pools: a comparative analysis of chlorophyll b and xanthophyll biosynthesis mutants. Molecular Plant **3,** 576–593.

Dekker JP, Boekema EJ. 2005. Supramolecular organization of thylakoid membrane proteins in green plants. Biochimica et Biophysica Acta **1706,** 12–39.

Demmig-Adams B. 1990. Carotenoids and photoprotection in plants: a role for the xanthophyll zeaxanthin. Biochimica et Biophysica Acta **1020,** 1–24.

Demmig-Adams B, Adams WW. 1992. Carotenoid composition in sun and shade leaves of plants with different life forms. Plant Cell and Environment **15,** 411–419.

Erickson E, Wakao S, Niyogi KK. 2015. Light stress and photoprotection in *Chlamydomonas reinhardtii*. The Plant Journal **82,** 449–465.

Garcia-Mendoza E, Ocampo-Alvarez H, Govindjee. 2011. Photoprotection in the brown alga *Macrocystis pyrifera*: evolutionary implications. Journal of Photochemistry and Photobiology. B, Biology **104,** 377–385.

Gilmore AM, Yamamoto HY. 1992. Dark induction of zeaxanthin-dependent nonphotochemical fluorescence quenching mediated by ATP. Proceedings of the National Academy of Sciences, USA **89,** 1899–1903.

Goss R, Jakob T. 2010. Regulation and function of xanthophyll cycle-dependent photoprotection in algae. Photosynthesis Research **106,** 103–122.

Goss R, Lepetit B. 2015. Biodiversity of NPQ. Journal of Plant Physiology **172,** 13–32.

Grossman AR, Karpowicz SJ, Heinnickel M, *et al*. 2010. Phylogenomic analysis of the *Chlamydomonas* genome unmasks proteins potentially involved in photosynthetic function and regulation. Photosynthesis Research **106,** 3–17.

Grouneva I, Jakob T, Wilhelm C, Goss R. 2008. A new multicomponent NPQ mechanism in the diatom *Cyclotella meneghiniana*. Plant & Cell Physiology **49,** 1217–1225.

Guillard RR, Ryther JH. 1962. Studies of marine planktonic diatoms. I. *Cyclotella nana* Hustedt, and *Detonula confervacea* (cleve) Gran. Canadian Journal of Microbiology **8,** 229–239.

Gundermann K, Büchel C. 2008. The fluorescence yield of the trimeric fucoxanthin-chlorophyll-protein FCPa in the diatom *Cyclotella meneghiniana* is dependent on the amount of bound diatoxanthin. Photosynthesis Research **95,** 229–235.

Gundermann K, Büchel C. 2012. Factors determining the fluorescence yield of fucoxanthin-chlorophyll complexes (FCP) involved in non-photochemical quenching in diatoms. Biochimica et Biophysica Acta **1817,** 1044–1052.

Horton P, Johnson MP, Perez-Bueno ML, Kiss AZ, Ruban AV. 2008. Photosynthetic acclimation: does the dynamic structure and macro-organisation of photosystem II in higher plant grana membranes regulate light harvesting states? The FEBS Journal **275,** 1069–1079.

Horton P, Ruban AV, Walters RG. 1996. Regulation of light harvesting in green plants. Annual Review of Plant Physiology and Plant Molecular Biology **47,** 655–684.

Horton P, Ruban AV, Wentworth M. 2000. Allosteric regulation of the light-harvesting system of photosystem II. Philosophical Transactions of the Royal Society of London. Series B, Biological Sciences **355,** 1361–1370.

Jahns P, Holzwarth AR. 2012. The role of the xanthophyll cycle and of lutein in photoprotection of photosystem II. Biochimica et Biophysica Acta **1817,** 182–193.

Jennings RC, Engelmann E, Garlaschi F, Casazza AP, Zucchelli G. 2005. Photosynthesis and negative entropy production. Biochimica et Biophysica Acta **1709,** 251–255.

Johnson MP, Goral TK, Duffy CD, Brain AP, Mullineaux CW, Ruban AV. 2011. Photoprotective energy dissipation involves the reorganization of photosystem II light-harvesting complexes in the grana membranes of spinach chloroplasts. The Plant Cell **23,** 1468–1479.

Johnson MP, Pérez-Bueno ML, Zia A, Horton P, Ruban AV. 2009. The zeaxanthin-independent and zeaxanthin-dependent qE components of nonphotochemical quenching involve common conformational changes within the photosystem II antenna in Arabidopsis. Plant Physiology **149,** 1061–1075.

Johnson MP, Ruban AV. 2011. Restoration of rapidly reversible photoprotective energy dissipation in the absence of PsbS protein by enhanced ΔpH. The Journal of Biological Chemistry **286,** 19973–19981.

Johnson MP, Zia A, Horton P, Ruban AV. 2010. Effect of xanthophyll composition on the chlorophyll excited state lifetime in plant leaves and isolated LHCII. Chemical Physics **373,** 23–32.

Johnson MP, Zia A, Ruban AV. 2012. Elevated ΔpH restores rapidly reversible photoprotective energy dissipation in *Arabidopsis* chloroplasts deficient in lutein and xanthophyll cycle activity. Planta **235,** 193–204.

Kaňa R, **Govindjee**. 2016. Role of ions in the regulation of light-harvesting. Frontiers in Plant Science **7,** 1–17.

Kaňa R, Kotabová E, KopeČná J, Trsková E, Belgio E, Sobotka R, Ruban AV. 2016. Violaxanthin inhibits nonphotochemical quenching in light-harvesting antenna of *Chromera velia*. FEBS Letters **590,** 1076–1085.

Kaňa R, Kotabová E, Sobotka R, Prášil O. 2012. Non-photochemical quenching in cryptophyte alga *Rhodomonas salina* is located in chlorophyll a/c antennae. PLoS One **7,** e29700.

Kaňa R, Vass I. 2008. Thermoimaging as a tool for studying light-induced heating of leaves: Correlation of heat dissipation with the efficiency of photosystem II photochemistry and non-photochemical quenching. Environmental and Experimental Botany **64,** 90–96.

Kirchhoff H, Haferkamp S, Allen JF, Epstein DB, Mullineaux CW. 2008. Protein diffusion and macromolecular crowding in thylakoid membranes. Plant Physiology **146,** 1571–1578.

Kotabová E, Kaňa R, Jarešová J, Prášil O. 2011. Non-photochemical fluorescence quenching in *Chromera velia* is enabled by fast violaxanthin de-epoxidation. FEBS Letters **585,** 1941–1945.

Kouřil R, Wientjes E, Bultema JB, Croce R, Boekema EJ. 2013. High-light vs. low-light: effect of light acclimation on photosystem II composition and organization in *Arabidopsis thaliana*. Biochimica et Biophysica Acta **1827,** 411–419.

Lavaud J, Kroth PG. 2006. In diatoms, the transthylakoid proton gradient regulates the photoprotective non-photochemical fluorescence quenching beyond its control on the xanthophyll cycle. Plant & Cell Physiology **47,** 1010–1016.

Lavaud J, Lepetit B. 2013. An explanation for the inter-species variability of the photoprotective non-photochemical chlorophyll fluorescence quenching in diatoms. Biochimica et Biophysica Acta **1827,** 294–302.

Lavaud J, Rousseau B, van Gorkom HJ, Etienne AL. 2002. Influence of the diadinoxanthin pool size on photoprotection in the marine planktonic diatom *Phaeodactylum tricornutum*. Plant Physiology **129,** 1398–1406.

Lepetit B, Volke D, Gilbert M, Wilhelm C, Goss R. 2010. Evidence for the existence of one antenna-associated, lipid-dissolved and two protein-bound pools of diadinoxanthin cycle pigments in diatoms. Plant Physiology **154,** 1905–1920.

Li XP, Björkman O, Shih C, Grossman AR, Rosenquist M, Jansson S, Niyogi KK. 2000. A pigment-binding protein essential for regulation of photosynthetic light harvesting. Nature **403,** 391–395.

Li XP, Gilmore AM, Caffarri S, Bassi R, Golan T, Kramer D, Niyogi KK. 2004. Regulation of photosynthetic light harvesting involves intrathylakoid lumen pH sensing by the PsbS protein. The Journal of Biological Chemistry **279,** 22866–22874.

Liguori N, Roy LM, Opacic M, Durand G, Croce R. 2013. Regulation of light harvesting in the green alga *Chlamydomonas reinhardtii*: the C-terminus of LHCSR is the knob of a dimmer switch. Journal of the American Chemical Society **135,** 18339–18342.

Lokstein H, Tian L, Polle JE, DellaPenna D. 2002. Xanthophyll biosynthetic mutants of *Arabidopsis thaliana*: altered nonphotochemical quenching of chlorophyll fluorescence is due to changes in Photosystem II antenna size and stability. Biochimica et Biophysica Acta **1553,** 309–319.

Mann M, Hoppenz P, Jakob T, Weisheit W, Mittag M, Wilhelm C, Goss R. 2014. Unusual features of the high light acclimation of *Chromera velia*. Photosynthesis Research **122,** 159–169.

Miloslavina Y, Wehner A, Lambrev PH, Wientjes E, Reus M, Garab G, Croce R, Holzwarth AR. 2008. Far-red fluorescence: a direct spectroscopic marker for LHCII oligomer formation in non-photochemical quenching. FEBS Letters **582,** 3625–3631.

Moya I, Silvestri M, Vallon O, Cinque G, Bassi R. 2001. Time-resolved fluorescence analysis of the photosystem II antenna proteins in detergent micelles and liposomes. Biochemistry **40,** 12552–12561.

Natali A, Gruber JM, Dietzel L, Stuart MC, van Grondelle R, Croce R. 2016. Light-harvesting complexes (LHCs) cluster spontaneously in membrane environment leading to shortening of their excited state lifetimes. The Journal of Biological Chemistry **291,** 16730–16739.

Nitschke U, Connan S, Stengel DB. 2012. Chlorophyll a fluorescence responses of temperate Phaeophyceae under submersion and emersion regimes: a comparison of rapid and steady-state light curves. Photosynthesis Research **114,** 29–42.

Niyogi KK. 1999. Photoprotection revisited: genetic and molecular approaches. Annual Review of Plant Physiology and Plant Molecular Biology **50,** 333–359.

Noctor G, Rees D, Young A, Horton P. 1991. The relationship between zeaxanthin, energy-dependent quenching of chlorophyll fluorescence,

and trans-thylakoid pH gradient in isolated chloroplasts. Biochimica et Biophysica Acta **1057,** 320–330.

Oborník M, KruČinská J, Esson H. 2016. Life cycles of chromerids resemble those of colpodellids and apicomplexan parasites. Perspectives in Phycology **3,** 21–27.

Obornik M, Lukes J. 2013. Cell biology of chromerids: autotrophic relatives to apicomplexan parasites. International Review of Cell and Molecular Biology **306,** 333–369.

Oborník M, Vancová M, Lai DH, Janouškovec J, Keeling PJ, Lukeš J. 2011. Morphology and ultrastructure of multiple life cycle stages of the photosynthetic relative of apicomplexa, *Chromera velia*. Protist **162,** 115–130.

Ocampo-Alvarez H, García-Mendoza E, Govindjee. 2013. Antagonist effect between violaxanthin and de-epoxidated pigments in nonphotochemical quenching induction in the qE deficient brown alga *Macrocystis pyrifera*. Biochimica et Biophysica Acta **1827,** 427–437.

Pan H, Slapeta J, Carter D, Chen M. 2012. Phylogenetic analysis of the light-harvesting system in *Chromera velia*. Photosynthesis research **111,** 19–28.

Pan X, Li M, Wan T, Wang L, Jia C, Hou Z, Zhao X, Zhang J, Chang W. 2011. Structural insights into energy regulation of light-harvesting complex CP29 from spinach. Nature Structural & Molecular Biology **18,** 309–315.

Peers G, Truong TB, Ostendorf E, Busch A, Elrad D, Grossman AR, Hippler M, Niyogi KK. 2009. An ancient light-harvesting protein is critical for the regulation of algal photosynthesis. Nature **462,** 518–521.

Peltier JB, Emanuelsson O, Kalume DE, *et al*. 2002. Central functions of the lumenal and peripheral thylakoid proteome of Arabidopsis determined by experimentation and genome-wide prediction. The Plant Cell **14,** 211–236.

Petrou K, Belgio E, Ruban AV. 2014. pH sensitivity of chlorophyll fluorescence quenching is determined by the detergent/protein ratio and the state of LHCII aggregation. Biochimica et Biophysica Acta **1837,** 1533–1539.

Pinnola A, Dall'Osto L, Gerotto C, Morosinotto T, Bassi R, Alboresi A. 2013. Zeaxanthin binds to light-harvesting complex stress-related protein to enhance nonphotochemical quenching in *Physcomitrella patens*. The Plant Cell **25,** 3519–3534.

Porra R, Thompson W, Kriedemann P. 1989. Determination of accurate extinction coefficients and simultaneous equations for assaying chlorophylls *a* and *b* extracted with four different solvents: Verification of the concentration of chlorophyll standards by atomic absorption spectrometry. Biochimica et Biophysica Acta **975,** 384–394.

Quigg A, Kotabová E, Jarešová J, Kaňa R, Setlík J, Sedivá B, Komárek O, Prášil O. 2012. Photosynthesis in *Chromera velia* represents a simple system with high efficiency. PLoS One **7,** e47036.

Ruban A. 2013. The photosynthetic membrane. Molecular mechanisms and biophysics of light harvesting. Chichester, UK: John Wiley & Sons, Ltd.

Ruban AV, Horton P. 1999. The xanthophyll cycle modulates the kinetics of nonphotochemical energy dissipation in isolated light-harvesting complexes, intact chloroplasts, and leaves of spinach. Plant Physiology **119,** 531–542.

Ruban AV, Johnson MP, Duffy CD. 2012. The photoprotective molecular switch in the photosystem II antenna. Biochimica et Biophysica Acta **1817,** 167–181.

Ruban A, Lavaud J, Rousseau B, Guglielmi G, Horton P, Etienne AL. 2004. The super-excess energy dissipation in diatom algae: comparative analysis with higher plants. Photosynthesis Research **82,** 165–175.

Ruban AV, Pesaresi P, Wacker U, Irrgang KD, Bassi R, Horton P. 1998. The relationship between the binding of dicyclohexylcarbodiimide and quenching of chlorophyll fluorescence in the light-harvesting proteins of photosystem II. Biochemistry **37,** 11586–11591.

Ruban AV, Rees D, Noctor GD, Young A, Horton P. 1991. Long-wavelength chlorophyll species are associated with amplification of high-energy-state excitation quenching in higher-plants. Biochimica et Biophysica Acta **1059,** 355–360.

Ruban AV, Young A, Horton P. 1994*a*. Modulation of chlorophyll fluorescence quenching in isolated light-harvesting complex of Photosystem-II. Biochimica et Biophysica Acta **1186,** 123–127.

Ruban AV, Young AJ, Pascal AA, Horton P. 1994*b*. The effects of illumination on the xanthophyll composition of the photosystem II light-harvesting complexes of spinach thylakoid membranes. Plant Physiology **104,** 227–234.

Serôdio J, Lavaud J. 2011. A model for describing the light response of the nonphotochemical quenching of chlorophyll fluorescence. Photosynthesis Research **108,** 61–76.

Schaller-Laudel S, Volke D, Redlich M, Kansy M, Hoffmann R, Wilhelm C, Goss R. 2015. The diadinoxanthin diatoxanthin cycle induces structural rearrangements of the isolated FCP antenna complexes of the pennate diatom *Phaeodactylum tricornutum*. Plant Physiology and Biochemistry **96,** 364–376.

Sobotka R, Esson HJ, Koník P, Trsková E, Moravcová L, Horák A, Dufková P, Oborník M. 2017. Extensive gain and loss of photosystem I subunits in chromerid algae, photosynthetic relatives of apicomplexans. Scientific Reports **7,** 13214.

Standfuss J, Terwisscha van Scheltinga AC, Lamborghini M, Kühlbrandt W. 2005. Mechanisms of photoprotection and nonphotochemical quenching in pea light-harvesting complex at 2.5 Å resolution. The EMBO Journal **24,** 919–928.

Tichy J, Gardian Z, Bina D, Konik P, Litvin R, Herbstova M, Pain A, Vacha F. 2013. Light harvesting complexes of *Chromera velia*, photosynthetic relative of apicomplexan parasites. Biochimica et Biophysica Acta **1827,** 723–729.

van Kooten O, Snel JF. 1990. The use of chlorophyll fluorescence nomenclature in plant stress physiology. Photosynthesis Research **25,** 147–150.

Walters RG, Ruban AV, Horton P. 1994. Higher plant light-harvesting complexes LHCIIa and LHCIIc are bound by dicyclohexylcarbodiimide during inhibition of energy dissipation. European Journal of Biochemistry **226,** 1063–1069.

Wentworth M, Ruban AV, Horton P. 2000. Chlorophyll fluorescence quenching in isolated light harvesting complexes induced by zeaxanthin. FEBS Letters **471,** 71–74.

Wientjes E, van Amerongen H, Croce R. 2013. Quantum yield of charge separation in photosystem II: functional effect of changes in the antenna size upon light acclimation. The Journal of Physical Chemistry B **117,** 11200–11208.

Xiao FG, Ji HF, Shen L. 2012. Insights into the region responding to ΔpH change in major light harvesting complex. Journal of Photochemistry and Photobiology. B, Biology **111,** 35–38.

Xu P, Tian L, Kloz M, Croce R. 2015. Molecular insights into Zeaxanthin-dependent quenching in higher plants. Scientific Reports **5,** 13679.

Zaks J, Amarnath K, Sylak-Glassman EJ, Fleming GR. 2013. Models and measurements of energy-dependent quenching. Photosynthesis Research **116,** 389–409.